



OPEN Enyne acetogenins from *Porcelia macrocarpa* displayed anti-*Trypanosoma cruzi* activity and cause a reduction in the intracellular calcium level

Fernanda Thevenard¹, Ivanildo A. Brito¹, Thais A. Costa-Silva^{1,3}, Andre G. Tempone²✉ & João Henrique G. Lago¹✉

Natural products are a promising source of new compounds with a wide spectrum of pharmacological properties, including antiprotozoal activities. Chagas disease, caused by the protozoan parasite *Trypanosoma cruzi*, is one of several neglected tropical diseases with reduced options for treatment, which presents limitations such as toxicity and ineffectiveness in the chronic stage of the disease. Aiming to investigate the Brazilian flora for the discovery of new anti-*T. cruzi* compounds, the MeOH extract from *Porcelia macrocarpa* R.E. Fries (Annonaceae) fruit peels displayed potent activity against trypomastigotes and intracellular amastigotes and was subjected to bioactivity-guided fractionation. Using different chromatographic steps, a fraction composed of a mixture of four new chemically related acetogenins was obtained. The compounds were characterized as (2*S**,3*R**,4*R**)-3-hydroxy-4-methyl-2-(*n*-octadeca-13',17'-dien-11'-inil)butanolide (1), (2*S**,3*R**,4*R**)-3-hydroxy-4-methyl-2-(*n*-eicosa-13',19'-dien-11'-inil)butanolide (2), (2*S**,3*R**,4*R**)-3-hydroxy-4-methyl-2-(*n*-octadec-13'-en-11'-inil)butanolide (3), and (2*S**,3*R**,4*R**)-3-hydroxy-4-methyl-2-(*n*-eicosa-13'-en-11'-inil)butanolide (4) by NMR analysis and UHPLC/ESI-HRMS data. The mixture of compounds 1–4, displayed an EC₅₀ of 4.9 and 2.5 µg/mL against trypomastigote and amastigote forms of *T. cruzi*, respectively, similar to the standard drug benznidazole (EC₅₀ of 4.8 and 1.4 µg/mL). Additionally, the mixture of compounds 1–4 displayed no mammalian toxicity for murine fibroblasts (CC₅₀ > 200 µg/mL), resulting in a SI > 40.8 and > 83.3 against trypomastigotes and amastigotes, respectively. Based on these results, the mechanism of action of this bioactive fraction was investigated. After a short-time incubation with the trypomastigotes, no alterations in the cell membrane permeability were observed. However, it was verified a decrease in the intracellular calcium of the parasites, without significant pH variations of the acidocalcisomes. The intracellular damages were followed by an upregulation of the reactive oxygen species and ATP, but no depolarization effects were observed in the mitochondrial membrane potential. These data suggest that the mixture of compounds 1–4 caused an irreversible oxidative stress in the parasites, leading to death. If adequately studied, these acetogenins can open new insights for the discovery of new routes of death in *T. cruzi*.

Chagas disease (CD) is a disease caused by the protozoan parasite *Trypanosoma cruzi*^{1,2}. Transmitted through some reduviid hematophagous insects, CD is endemic to South and Central America, with vector-borne and oral as primary forms of transmission in these regions³. Due to globalization and human migration, the incidence of this disease increased in urban centers and in non-endemic countries where the principal transmission form is congenital or vertical transmission^{4–7}. This disease presents two clinical phases: an acute phase, mostly asymptomatic and with a high blood parasitemia caused by the trypomastigote forms. The chronic phase is characterized by the presence of intracellular amastigotes and 30% of cases can progress to heart/digestive tract mega-syndromes and is the major cause of cardiac diseases in endemic areas^{3,8–10}. Infecting more than seven

¹Centre for Natural and Human Sciences, Federal University of ABC, São Paulo, Brazil. ²Centre for Parasitology and Mycology, Instituto Adolfo Lutz, São Paulo, Brazil. ³SENAI Institute of Innovation in Biotechnology, São Paulo 01130-000, Brazil. ✉email: andre.tempone@ial.sp.gov.br; joao.lago@ufabc.edu.br

million people worldwide, an estimated seven million are affected in Latin America where being about one million women of reproductive age^{1,10}. It is assumed that CD causes about US\$ 7 billion/year in production loss, cardiovascular disease treatment, and health care worldwide within US\$ 1 billion only in South America^{5,6}. Due to a low investment, there are only two drugs available for the clinical treatment, benznidazole and nifurtimox, with efficacy restricted to the acute phase and intense side effects^{10,11}. Since cardiac and gastro-intestinal patients are especially susceptible to COVID-19 complications, the outbreak increases the urgency for new drugs and treatments, especially due to impacted health services, and worsening prognostics^{12–15}.

In this context, natural products are an alternative in the prospection of new drug prototypes¹⁶. Previous studies from our research group with *Porcelia macrocarpa* R.E. Fries (Annonaceae) led to the isolation of metabolites with in vitro potential against trypanostigote and amastigote forms of *T. cruzi*. As reported^{17,18}, extracts from seeds and flowers afforded acetylene acetogenins and fatty acids with potent activity against trypanostigotes forms of *T. cruzi* caused by depolarization of both the plasma membrane and mitochondrial membrane potential of the parasite. As part of our continuous studies with this plant, the MeOH extract from fruits peels of *P. macrocarpa* was prepared and the effect against trypanostigotes and amastigotes of *T. cruzi* was investigated. As a result, it was observed that this extract caused 100% of parasite death at 300 µg/mL indicating the presence of bioactive metabolites. Using a bioactivity-guided approach, it was obtained a fraction composed of a mixture of four new enyne acetogenins (1–4) which were chemically characterized by NMR and UHPLC/ESI-HRMS and evaluated against *T. cruzi* trypanostigotes and amastigotes. Finally, insight into the mechanism of lethal action of the mixture composed by 1–4 was investigated.

Results and discussion

Chemical characterization of compounds 1–4. Bioactive fraction D-1 obtained by chromatographic fractionation of MeOH extract from *P. macrocarpa* (see “Methodology” section) fruit peels was analyzed by UHPLC/UV analysis. As could be seen in Fig. 1, this fraction showed to be composed of four related compounds (1–4) due to the absorptions at λ_{\max} at 212, 267 and 283 nm. According with literature data¹⁹, this profile is characteristic of enyne conjugated system. Molecular formulas for these compounds were established as C₂₃H₃₆O₃ (1, [M + H]⁺ and [M + Na]⁺ at *m/z* 361.2740 and 383.2560), C₂₅H₄₀O₃ (2, [M + H]⁺ and [M + Na]⁺ at *m/z* 389.3054 and 411.2877), C₂₃H₃₈O₃ (3, [M + H]⁺ and [M + Na]⁺ at *m/z* 363.2893 and 385.2722) and C₂₅H₄₂O₃ (4, [M + H]⁺ and [M + Na]⁺ at *m/z* 391.3210 and 413.3034) by ESI-HRMS (Fig. 1). ¹H NMR spectra of mixture of compounds 1–4 displayed characteristic signals of a γ -lactone ring at δ_{H} 1.43 (d, *J* = 6.5 Hz, H-5), 2.58 (dt, *J* = 4.8 e 3.0 Hz, H-2), 4.31 (dd, *J* = 4.8 e 3.0 Hz, H-3), and 4.46 (dq, *J* = 6.5 e 3.0 Hz, H-4)^{18,19}. Signals attributed to hydrogens of a terminal double bond of an alkyl side chain at δ_{H} 5.82 (ddt, *J* = 16.9, 9.9 e 6.8 Hz, H-19' for 2 and H-17' for 1) and 4.97 (m, H-20' for 2 and H-18' for 1) were observed. However, the presence of a triplet at δ_{H} 0.88 (*J* = 6.9 Hz, H-20' for 4 and H-18' for 3), assigned to a terminal methyl group, suggested the presence of related derivatives but containing a sp³ carbon at terminal position of side chain, similar of related γ -lactones isolated from seeds of *P. macrocarpa*²⁰. Interestingly, ¹H NMR spectrum showed additional signals at δ_{H} 6.04 (dt, *J* = 10.7 e 7.6 Hz) and δ_{H} 5.48 (t, *J* = 10.7 Hz) attributed, respectively, to hydrogens of an enyne conjugation system, in agreement with data obtained from UV spectrum.^{19,20} ¹³C and DEPT NMR spectra confirmed this proposal, with signals referring to the γ -lactone ring at δ_{C} 177.5 (C-1), 47.6 (C-2), 71.3 (C-3), 78.7 (C-4), and 13.7 (H-5). Signals at δ_{C} 80.1 and 80.2 were attributed, respectively, to sp carbons C-13' and C-14' whereas those at δ_{C} 137.6 and 115.2

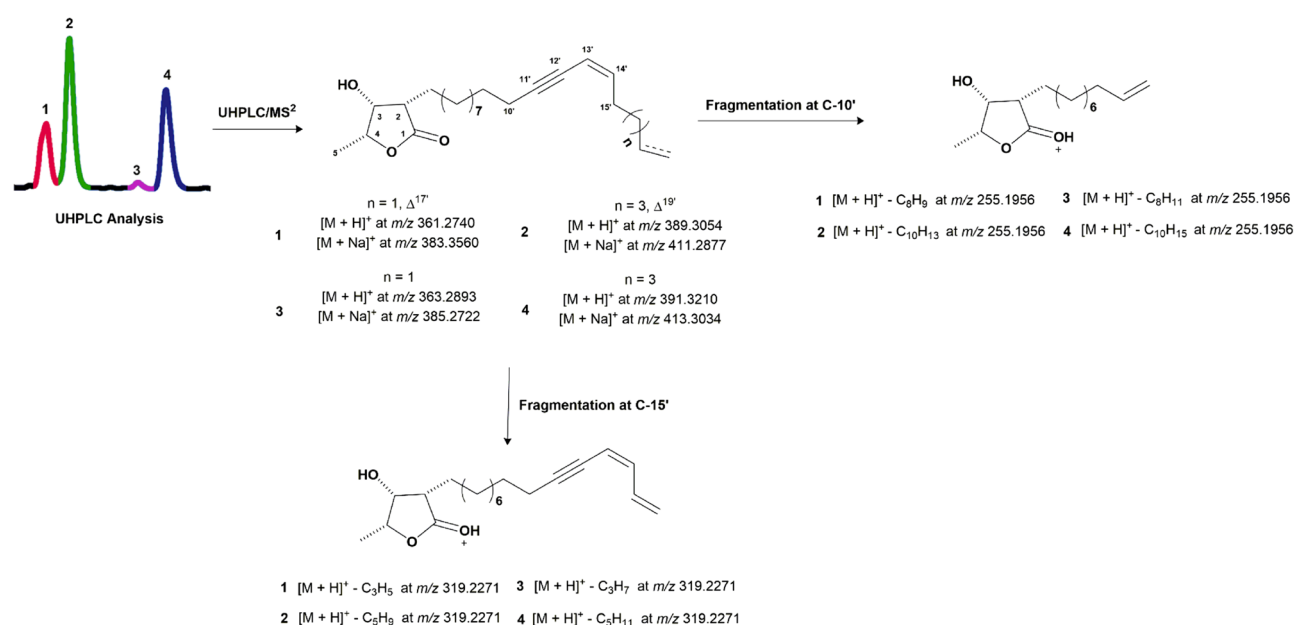


Figure 1. UHPLC-ESI-HRMS/MS (positive mode) analysis of bioactive fraction D-1 from *P. macrocarpa* fruit peels and structures of acetogenins 1–4.

were assigned to sp² carbons in Z configuration—C-16' and C-15', respectively—in order to confirm the presence of enyne system. Furthermore, signals at δ_C 139.2 (C-19' for **2** and C-17' for **1**) and 114.5 (C-20' for **4** and C-18' for **3**), attributed to the terminal double bonds, were also observed. Additionally, these spectra showed a signal at δ_C 14.1 (C-20' for **4** and C-18' for **3**) confirming the presence of derivatives containing terminal methyl group. The positioning of conjugated triple and double bonds on the alkyl side chain for compounds **1–4** was determined at C-11' and C-13', respectively, through MS/MS analysis which exhibited fragments of C-10'/C11' at m/z 255.1957 and of C-15'/C-16' at m/z 319.2270, as showed in Fig. 1. Finally, the relative configuration of γ -lactone ring was determined as *cis,cis,cis* based on values of chemical shifts to carbons C-1, C-2, C-3 and C-4, as observed for chemically related other acetogenins obtained from seeds of *P. macrocarpa*²⁰. Therefore, structures of new compounds **1–4** were elucidated as (2S*,3R*,4R*)-3-hydroxy-4-methyl-2-(*n*-octadeca-13',17'-dien-11'-inil)butanolide (**1**), (2S*,3R*,4R*)-3-hydroxy-4-methyl-2-(*n*-eicosa-13',19'-dien-11'-inil)butanolide (**2**), (2S*,3R*,4R*)-3-hydroxy-4-methyl-2-(*n*-octadec-13'-en-11'-inil)butanolide (**3**), and (2S*,3R*,4R*)-3-hydroxy-4-methyl-2-(*n*-eicosa-13'-en-11'-inil)butanolide (**4**).

Anti-*T. cruzi* activity. The mixture of compounds **1–4** (fraction D-1) displayed EC₅₀ values of 4.9 and 2.5 μ g/mL against trypomastigotes and intracellular amastigotes, respectively (Table 1), similar to the values obtained for the standard drug, benznidazol (EC₅₀=4.8 and 1.4 μ g/mL, respectively). No cytotoxicity was observed against mammalian NCTC cells to the highest tested concentration (CC₅₀>200 μ g/mL). The mixture of compounds **1–4** showed elevated selectivity indexes for the bloodstream form (SI>40.8) and for the intracellular form (SI>83.3) of the parasite. Comparatively, the standard drug benznidazole resulted in SI>10.8 for trypomastigotes and >36.4 for amastigotes. Previous studies¹⁸ evaluated the effect of related acetogenins from seeds of *P. macrocarpa* and compounds with same γ -lactone unity, but containing a side chain with a triple bond at C-11' and one double bond at C-19' displayed moderate activity against amastigotes. Otherwise, no effects against *T. cruzi* were observed when a saturated side chain was present, indicating that unsaturation is a crucial feature for the antiparasitic activity. As observed in this work, the effect of the mixture of acetogenins **1–4** against *T. cruzi* was quite similar to the standard drug benznidazole. This data demonstrates that the presence of the enyne conjugated system plays an important role in the potential against the parasite. Therefore, due to the high activity and improvement of SI when compared to benznidazole, the fraction composed by **1–4** was subjected to further biological studies to evaluate its mechanism of action against trypomastigotes of *T. cruzi*.

Mechanisms of action studies. The lethal mechanisms of the fraction D-1, containing compounds **1–4**, was performed to evaluate the plasma membrane permeability, the analysis of intracellular calcium levels, the acidocalcisome alkalization and mitochondrial membrane alterations, including the electric potential, reactive oxygen species and the ATP levels.

Plasma membrane permeability. The plasma membrane regulates transport of ions and nutrients as well as pH and other factors²¹. As such, alterations in its composition can modify the fluidity and contribute to trypomastigote death²². Amphotericin B, a clinical drug used in the treatment of *Leishmania* spp., causes permeabilization of the plasma membrane of this protozoan parasite²³. To evaluate this effect we incubated the mixture of compounds **1–4** (fraction D-1) with trypomastigotes for up to 120 min at the EC₅₀ value of 4.9 μ g/mL and detected alterations in the fluorescence levels using Sytox Green, a fluorescent probe that binds to nucleic acids and increases the fluorescence after membrane damages²⁴. Triton X-100, a non-ionic detergent, was used as a positive control to induce the solubilization of the lipid bilayer²⁵. No increases in fluorescence levels were observed after treatment with the mixture of compounds **1–4** (Fig. 2), suggesting no effect in the membrane of the parasite.

Intracellular Ca²⁺ levels. Calcium ions regulate several signalization pathways, parasite differentiation, flagellar function and are essential for trypanosomatids survival. Alteration of calcium homeostasis can result in the parasite death^{26,27}. Using the fluorescent probe Fluo-4AM dye, it was observed that the mixture of compounds **1–4** (fraction D-1) caused reduction of cytosolic Ca²⁺ levels at all evaluated times of the incubation (Fig. 3), suggesting a metabolic imbalance. To evaluate the intracellular calcium, a known organelle in trypanosomatids was studied, named acidocalcisomes.

Acidocalcisome alkalization. Acidocalcisomes are acidic organelles and the main Ca²⁺ storage for trypanosomatids, where the ion is bound to polyphosphates^{27,28}. The alkalization of these organelles has been related to leakage of calcium to the cytoplasm²⁶. No effect was observed after treatment with the mixture of compounds **1–4**

Tested material	^a EC ₅₀ (μ g/mL)		^b CC ₅₀ (μ g/mL)	^c SI	
	Trypomastigotes	Amastigotes	NCTC	Trypomastigotes	Amastigotes
Fraction D-1 (mixture of compounds 1–4)	4.9 ± 0.8	2.5 ± 1.0	>200	>40.8	>83.3
Benznidazol (positive control)	4.8 ± 1.1	1.4 ± 0.6	>52.0	>10.8	>36.4

Table 1. Anti-*T. cruzi* activity and cytotoxicity of mixture of acetogenins **1–4** (fraction D-1) from *P. macrocarpa* fruit peels and positive control benznidazol. ^aEC₅₀, 50% effective concentration; ^bCC₅₀, 50% cytotoxic concentration; ^cSI, selectivity index (CC₅₀ mammalian cells/EC₅₀ parasite form).

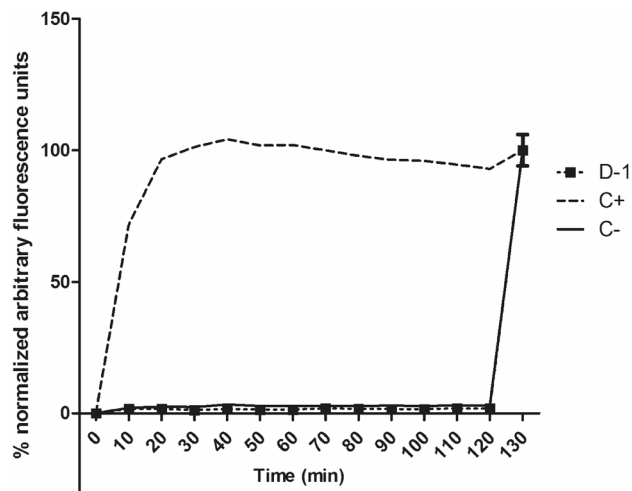


Figure 2. Evaluation of cell membrane permeability effects of the mixture of compounds 1–4 (fraction D-1) from *P. macrocarpa* fruit peels at the EC_{50} value of 4.9 $\mu\text{g}/\text{mL}$ in *T. cruzi* trypomastigotes. Sytox Green dye (excitation and emission wavelengths of 485 and 520 nm) was used, and fluorescence was monitored until 130 min. Untreated parasites (C–) and Triton X 100 (C+) were used for minimum and maximum permeabilization, respectively. A representative assay is shown.

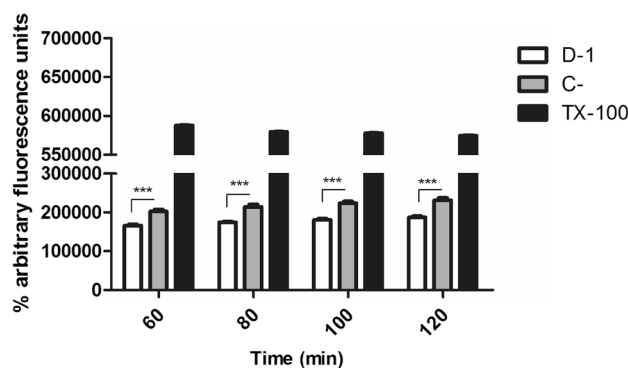


Figure 3. Effect of the mixture of compounds 1–4 (fraction D-1) from *P. macrocarpa* fruit peels on intracellular calcium levels in *T. cruzi* trypomastigotes. Using Fluo-4AM dye (excitation and emission wavelengths of 485 nm and 535, respectively), parasites were treated with I for 60, 80, 100 and 120 min at the EC_{50} value of 4.9 $\mu\text{g}/\text{mL}$. Positive (C+) and negative (C–) controls were Triton X-100 (0.5% v/v) and untreated parasites, respectively. Fluorescence in arbitrary units at each time point. A representative assay is shown. *** $p < 0.0001$.

(fraction D-1—Fig. 4), corroborating the reduction of calcium levels in the cytoplasm as previously observed. After treatment with the mixture of compounds 1–4, the decrease of the calcium levels in the cytoplasmic milieu of the parasite may be a result of the influx of this ion to the mitochondria or the endoplasmic reticulum, since both organelles are natural reservoirs of calcium in the parasite^{27,28}. Considering that an elevated concentration of calcium can harm the mitochondria²⁹, the electric potential of this vital organelle was further investigated.

Mitochondrial membrane potential ($\Delta\psi_m$). The single mitochondrion is unique to the trypanosomatids and is essential for the bioenergetic metabolism. It is also involved in calcium homeostasis as a known source of reactive oxygen species (ROS). Due to these characteristics, the *T. cruzi* mitochondria has been considered an interesting target for new anti-trypanosomal drugs^{29,30}. Compounds that affect the respiratory chain tend to impact the ROS production and can also induce oxidative stress. Using the JC-1 probe, alterations in the mitochondrial membrane potential were evaluated. As result, no decreases of the fluorescence levels were detected after treatment with the mixture of compounds 1–4 (fraction D-1—Fig. 5), when compared to untreated parasites. This data reflects no direct impact of the compounds to the organelle. It has been shown that the overloading of calcium by the mitochondria can affect the mitochondrial membrane potential³¹, but this effect was not observed after treatment with the mixture of compounds 1–4. Although no electric alterations were detected in the mitochondria, alterations of reactive oxygen species levels were studied.

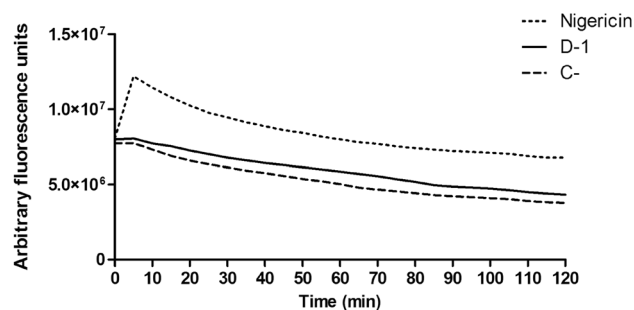


Figure 4. Time dependent analysis of acidocalcisome alkalization of *T. cruzi* trypomastigotes treated with the mixture of compounds 1–4 (fraction D-1) from *P. macrocarpa* fruit peels. Pretreatment with acridine orange dye (4 μ M) was performed before treating the parasites with the mixture of compounds 1–4 for 120 min at the EC₅₀ value of 4.9 μ g/mL. Nigericin (4 μ M) and non-treated parasites were the positive (C+), and negative (C–) control, respectively. A representative assay is shown.

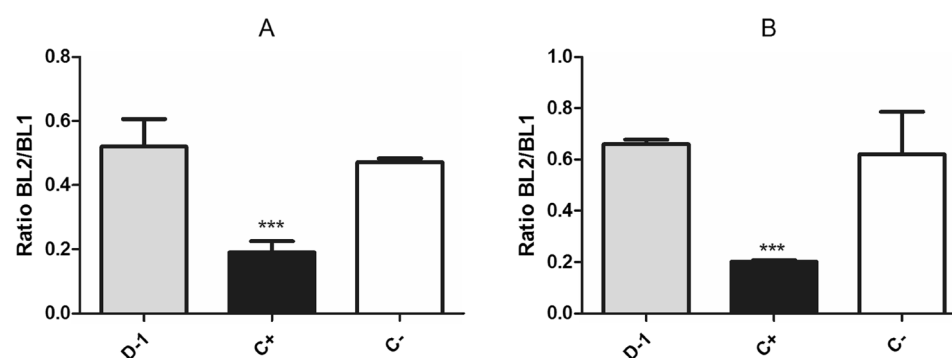


Figure 5. Effect of the mixture of compounds 1–4 (fraction D-1) from *P. macrocarpa* fruit peels on the mitochondrial membrane potential of *T. cruzi* trypomastigotes. Parasites were treated with the mixture of compounds 1–4 at 4.9 μ g/mL for 1 h (A) and 2 h (B), using JC-1 dye (excitation and emission wavelengths of 488 nm and 530/574 nm, respectively). Parasites treated with CCCP and untreated parasites were the positive (C+) and negative (C–) controls, respectively. A representative assay is shown. *** $p < 0.0002$.

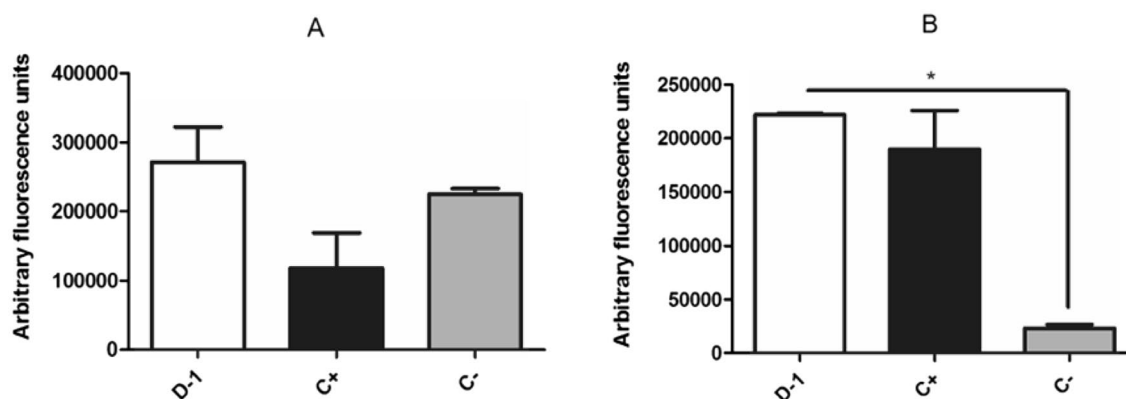


Figure 6. Effect of the mixture of compounds 1–4 (fraction D-1) from *P. macrocarpa* fruit peels on the levels of reactive oxygen species in *T. cruzi* trypomastigotes. H2DCFDA dye (excitation and emission wavelengths of 485 nm and 520 nm, respectively) was used in parasites treated with the mixture of compounds 1–4 at the EC₅₀ value of 4.9 μ g/mL for 1 h (A) and 2 h (B). Positive control (C+) was 10 mM azide and untreated *T. cruzi* was the negative control (C–). * $p < 0.01$.

Reactive oxygen species levels (ROS). The levels of ROS were also investigated after treatment with the mixture of compounds 1–4 (fraction D-1). Using the fluorescent probe H₂DCFDA, a significant ($p < 0.05$) increase in ROS levels was observed after 2 h of incubation (Fig. 6). Despite no statistical differences, the ROS levels were clearly increased after 1 h incubation when compared to the untreated parasites. Besides the cellular membrane, endoplasmic reticulum and the cytoplasm, the mitochondria contribute to 90% of the ROS production. The imbalance between mitochondrial reactive oxygen species and removal due to overproduction of ROS and/or decreased antioxidants defense activity results can cause the oxidative stress. These molecules can damage several cellular constituents as DNA, proteins and lipids³². Additionally, the detoxification of ROS in Trypanosomatids are done by thiols and the enzyme trypanothione reductase. When these systems fail to cope with an excessive production, these highly reactive molecules (ROS) can induce an oxidative stress, leading to a cellular death³². Due to this toxic effect after treatment with the mixture of compounds 1–4, we investigated the ATP levels.

ATP levels. Considering the increased levels of ROS and the possible damages caused by these highly reactive compounds, we investigated the ATP levels of the parasite using a luminescent assay with luciferin. The mixture of compounds 1–4 (fraction D-1) caused a significant increase in ATP levels after 1 h of treatment (Fig. 7) when compared to untreated cells. In parallel, ROS upregulation was also observed after 1 h of incubation as previously discussed (Fig. 6). Increased levels of ROS have been accompanied by elevated release of ATP³³. Mitochondrial oxidative phosphorylation is the major ATP synthetic pathway in eukaryotes, including Trypanosomatids. During this process, the reduction of O₂ molecules produces several reactive oxygen species (ROS)³⁴. It has also been known that Ca²⁺ is a physiological stimulus for ATP synthesis and consequently, a stimulus for ROS generation³⁴. Considering the tight connection among these metabolic compounds, the alteration of any of them can naturally affect the production of the other. In our studies, it is possible that the increased levels of ATP can be a cellular effort to fight the oxidative stress caused by the treatment with the mixture of compounds 1–4.

Conclusions

Using a bioactivity-guided approach, four new chemically related acetogenins 1–4 were characterized from the fraction D-1 obtained from the MeOH extract of *P. macrocarpa* fruit peels by NMR and UHPLC/ESI-HRMS analysis. The mixture of compounds 1–4 displayed anti-trypanosomal activity against trypomastigote and amastigote forms of the parasite with a similar effect to the standard drug benznidazole. Additionally, these new compounds showed no cytotoxicity against NCTC cells, demonstrating a promising potential. Due to this activity, mechanism of action studies were performed. The fraction containing compounds 1–4 reduced the cytosolic calcium levels, with no alkalization of the acidocalcisomes. Although it induced no depolarization of the mitochondrial membrane potential, increased levels of ATP were detected, as a possible cellular effect to counterbalance the oxidative stress caused by the elevated ROS levels leading to the parasite death.

Methodology

General experimental procedures. Silica gel 60 PF₂₅₄ (Merck—Darmstadt, Germany) was used for thin layer chromatography (TLC) whereas column chromatography (CC) procedures was performed using silica gel 60 (Merck—Darmstadt, Germany) or Sephadex LH-20 (Sigma-Aldrich—St. Louis, MO, USA). NMR spectra were obtained on a Varian Unity INOVA (500 MHz ¹H and 125 MHz ¹³C) using CDCl₃ as solvent and TMS as internal standard. Chemical shifts (δ) are given in ppm with coupling constants (J) in Hz. UHPLC experiments were performed on a ThermoScientific Ultimate 3000 model with DAD detector (UVD-170 model) and separation was performed on a Kinetex[®] C₁₈ analytic column (5 μ m–250 \times 4.6 mm) using ACN:H₂O 85:15 as eluent

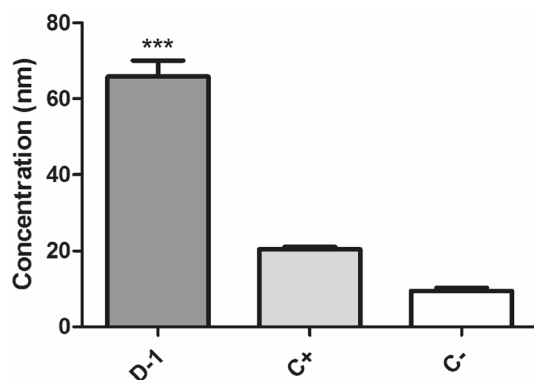


Figure 7. Evaluation of the ATP levels of *T. cruzi* trypomastigotes after treatment with the mixture of compounds 1–4 (fraction D-1) from *P. macrocarpa* fruit peels. ATP concentration was measured in a luminometer after 1 h parasite incubation with the mixture of compounds 1–4 at the EC₅₀ value of 4.9 μ g/mL. Negative (C⁻) and positive (C⁺) control were untreated parasites and trypomastigotes treated with 100 μ M CCCP, respectively. *** $p < 0.0001$.

at 1.0 mL/min. ESI-HRMS were measured on a Bruker Daltonics MicroTOF QII operating with electrospray ionization (positive mode).

Plant material. Fruits of *P. macrocarpa* were collected at the *Instituto de Botânica* in São Paulo city, São Paulo State, Brazil (23°38'33.8"S and 46°37'17.5"W) in 2017. Dr. Maria Claudia M. Young identified the plant material, and a voucher specimen was compared with that under number SP76791. This study was registered on the National System for the Management of Genetic Heritage and Associated Traditional Knowledge (SisGen) from the Ministry of the Environment, Brazil, under code A483B45. Experimental research and field studies on plants (either cultivated or wild), including the collection of plant material have complied with relevant institutional, national, and international guidelines and legislation.

Extraction and bioactivity-guided fractionation. The fruit peels were removed immediately after collection and dried at room temperature. After milling, the plant material (168 g) was defatted (10 × 1L) with *n*-hexane. The residual material was then extracted with MeOH (8 × 1L) at room temperature. After elimination of the solvent under reduced pressure, was obtained the MeOH extract (35 g) which was resuspended in MeOH:H₂O 1:1 and successively partitioned using *n*-hexane and EtOAc. As both crude MeOH extract and *n*-hexane phase displayed activity against *T. cruzi* (100% of parasite death at 300 µg/mL), part of the *n*-hexane phase (5 g) was fractionated over SiO₂ column chromatography eluted with increasing amounts of EtOAc in hexane to afford 10 fractions (A–J). Bioactive fraction D (1 g) was chromatographed over Sephadex LH-20 eluted with *n*-hexane:CH₂Cl₂ (1:4) and CH₂Cl₂:acetone (3:2 and 1:4) to afford eight groups (D-1 to D-8). Fraction D-1 (18 mg) displayed activity against *T. cruzi* and showed to be composed of a mixture of compounds 1–4 by NMR and UHPLC/ESI-HRMS analysis.

Bioassay procedures. *Animals.* BALB/c mice were utilized for *T. cruzi* maintenance infection and peritoneal macrophage collection³⁵. The mice were obtained from the animal breeding facility at the *Instituto Adolfo Lutz*—São Paulo, Brazil and maintained in sterilized boxes with absorbent material under a controlled environment. Food and water were given ad libitum. Procedures were approved by the Ethics Committee of the Instituto Adolfo Lutz (Project CEUA-IAL/Pasteur05/2018), in agreement with the Guide for the Care and Use of Laboratory Animals from the National Academy of Sciences.

Parasite and mammalian cell maintenance. Trypomastigotes (Y strain) were maintained in rhesus monkey kidney cells (LLC-MK2—ATCC CCL 7) using RPMI-1640 medium supplemented with 2% bovine fetal serum (BFS) in an incubator humidified with 5% CO₂ at 37 °C. LLC-MK2 and conjunctive mice cells (NCTC clone L929, ATCC) were maintained at 37 °C with RPMI-1640 supplemented with 10% fetal bovine serum at 5% CO₂. Macrophages were obtained from the peritoneal cavities of BALB/c mice through washing with the same medium^{36,37}.

In vitro activity against *trypomastigote* forms of *T. cruzi*. Trypomastigotes were obtained from previously infected LLC-MK2 cultures and counted in a Neubauer hemocytometer seeded at 1 × 10⁶ cells/well (96 well plates). The mixture of compounds 1–4 (fraction D-1) was added in serial dilution (100–1.6 µg/mL) using RPMI-1640 medium and the plated were incubated for 24 h at 37 °C in a 5% CO₂-humidified incubator. Benznidazole was used as the standard drug. Trypomastigote viability was evaluated by the resazurin assay^{17,36}.

In vitro activity against amastigote forms of *T. cruzi*. Previously obtained macrophages were plated on 16 well chamber slides (NUNC®, Merck) at 1 × 10⁵ macrophage/well and incubated for 24 h at 37 °C in a 5% CO₂-humidified incubator. Trypomastigotes were washed with RPMI-1640 medium and used to infect the cells at 1 × 10⁶/well for 2 h. After this time, non-internalized parasites were removed by washing with RPMI-1640 medium. Serial dilutions (100–1.6 µg/mL) of the mixture of compounds 1–4 (fraction D-1) were incubated with infected macrophages for 48 h at 37 °C and 5% CO₂ with benznidazole as the standard drug. Slides were then fixed with MeOH and stained with Giemsa. EC₅₀ values were obtained after counting infected cells with an light microscope (EVOS M5000) and calculated according to literature^{35,37}.

Cytotoxicity against mammalian cells and selectivity index determination. Cytotoxicity was evaluated against NCTC cells (L929 clone). Cells were incubated at 6 × 10⁴/well with serial dilutions (200–1.6 µg/mL) of the mixture of compounds 1–4 (fraction D-1) in RPMI medium supplemented with 10% BFS (48 h, 37 °C, 5% CO₂). CC₅₀ values were obtained by MTT assay. Optical density was determined by fluorimetric microplate reader (FilterMax F5, MolecularDevices) at a wavelength of 570 nm³⁵. Selectivity indexes (SI) for both forms of *T. cruzi* were calculated using the ratio—SI = CC₅₀ against NCTC cells/EC₅₀ against parasite forms.

Mechanism of action studies. *SYTOX Green assay for cell membrane permeability.* Washed trypomastigotes (2 × 10⁶/well) were incubated with 1 µM SYTOX Green probe (Molecular Probes) in HANKS' balanced salt solution (HBSS, Sigma-Aldrich) supplemented with 10 mM D-Glucose in the dark. The mixture of compounds 1–4 (fraction D-1) was added (t = 0 min) at the EC₅₀ value of 4.9 µg/mL and the fluorescence levels were measured every 20 min for 120 min. Untreated parasites were the negative control and maximum permeabilization was achieved with 0.5% Triton X-100. Fluorescence intensity was determined by fluorometric microplate reader (FilterMax F5) with excitation and emission wavelengths of 485 and 520 nm, respectively. Triton X-100 was added to all samples at the end of the assay.

Measurement of intracellular calcium (Ca²⁺) levels. Trypomastigotes (2 × 10⁶/well) were pre-treated with Fluo-4AM dye (5 µM) in Phosphate Buffer Solution (PBS) at 37 °C in the dark, for 1 h. Parasites were then briefly

washed and treated with the mixture of compounds 1–4 (fraction D-1) at the EC₅₀ value of 4.9 µg/mL. Using a fluorometric microplate reader (FilterMax F5 Multi-mode, Molecular Devices), fluorescence levels were measured for 260 min (485 and 535 nm for excitation and emission wavelengths, respectively). Negative control consisted of untreated parasites and maximum intracellular calcium levels were obtained using 0.5% Triton X-100 (v/v)^{38,39}.

Alterations in acidocalcisomes. Trypomastigotes (2 × 10⁶/well in 96 well plates) were washed with PBS and incubated with acridine orange dye (Thermo Fisher Scientific) at 4 µM for 5 min in the dark. Non-internalized probe was removed with PBS. The mixture of compounds 1–4 (fraction D-1) was incubated with the parasite at the EC₅₀ value of 4.9 µg/mL for 120 min. Fluorescence levels were measured using Multimode FilterMax F5 (Molecular Devices) microplate reader with excitation and emission wavelengths of 485 and 535 nm, respectively. Nigericin (4 µM) was used as positive control and non-treated parasites as negative control³⁹.

Mitochondrial membrane potential (Δψ_m). Trypomastigotes (2 × 10⁶/tube) were washed with HBSS supplemented with NaHCO₃ and D-glucose and incubated with the mixture of compounds 1–4 (fraction D-1) at the EC₅₀ value of 4.9 µg/mL, at 37 °C and 5% CO₂ for 1 and 2 h. After washing, JC-1 dye (10 µM) was added and the parasites were incubated for 20 min at 37 °C in the dark. Fluorescence was measured in a Attune NxT flow cytometer (488 and 530/574 nm excitation and emission wavelengths, respectively). The mitochondrial membrane potential was determined by the ratio between red/green fluorescence intensities (BL-2/BL-1). Positive and negative control were CCCP (Sigma-Aldrich) at 100 µM and non-treated parasites, respectively³⁹.

Measurement of ROS levels. The mixture of compounds 1–4 (fraction D-1) was incubated at the EC₅₀ value of 4.9 µg/mL with washed trypomastigotes (2 × 10⁶/well) in black 96 well plates in HBSS supplemented with NaHCO₃ (4.2 mM) and D-glucose (10 mM), at EC₅₀ value for 1 and 2 h (24 °C, 5% CO₂). Azide (10 µM) and untreated parasites were used as positive and negative controls, respectively. Afterwards, H₂DCFDA (20 µM) was incubated with the parasites for 15 min at 37 °C. Fluorescence intensity was measured using FilterMax F5 microplate reader (485 and 520 nm excitation and emission wavelengths, respectively). Controls containing only the compound and the fluorophore were added in all experiments to measure interference^{40,41}.

Measurement of ATP levels. The mixture of compounds 1–4 (fraction D-1) was incubated at the EC₅₀ value of 4.9 µg/mL with trypomastigotes (2 × 10⁶/well) in HBSS and glucose for 1 h, at 37 °C. Parasites were lysed with 0.5% Triton X-100 and mixed with a standard reaction buffer (ATP Determination kit—Thermo Fisher) containing DTT (1 mM), luciferin (0.5 mM) and luciferase (1.25 µg/mL). A luminometer (FilterMax F5 Multi-mode, Molecular Devices) was used for measuring luminescence intensity and ATP quantity calculated with an ATP standard curve³⁹.

Statistical analysis. Samples were tested in duplicates of three independent assays. Calculation of EC₅₀ and CC₅₀ values was performed using dose–response sigmoid curves in Graph-Pad Prism (GraphPad Prism software 6.0, San Diego, CA, USA). Mechanism of active studies were analyzed using ANOVA turkey test for significance (*p* < 0.05)³⁸.

Data availability

The datasets used and/or analyzed during the current study available from the corresponding author on reasonable request.

Received: 1 March 2023; Accepted: 22 June 2023

Published online: 24 June 2023

References

1. Chagas disease (also known as American trypanosomiasis). <https://www.who.int/news-room/fact-sheets/detail/chagas-disease-american-trypanosomiasis>. Accessed 09 Apr 2022.
2. Doença de Chagas | DNDi América Latina. <https://www.dndial.org/doencas/doenca-chagas/>.
3. Echeverría, L. E. *et al.* WHF IASC roadmap on chagas disease. *Glob. Heart* **15**(1), 26 (2020).
4. Schaub, G. A. An update on the knowledge of parasite–vector interactions of Chagas disease. *Res. Rep. Trop. Med.* **12**, 63–76 (2021).
5. Lidani, K. C. F. *et al.* Chagas disease: From discovery to a worldwide health problem. *Front. Public Health* **7**, 166 (2019).
6. Lascano, F., García Bournissen, F. & Altcheh, J. Review of pharmacological options for the treatment of Chagas disease. *Br. J. Clin. Pharmacol.* **88**(2), 383–402 (2022).
7. Abras, A. *et al.* Worldwide control and management of Chagas disease in a new era of globalization: A close look at congenital *Trypanosoma cruzi* infection. *Clin. Microbiol. Rev.* **35**(2), e00152–e221 (2022).
8. Alonso-Padilla, J. *et al.* Strategies to enhance access to diagnosis and treatment for chagas disease patients in latin America. *Expert Rev. Anti Infect. Ther.* **17**(3), 145–157 (2019).
9. García-Huertas, P. & Cardona-Castro, N. Advances in the treatment of Chagas disease: Promising new drugs, plants and targets. *Biomed. Pharmacother.* **142**, 112020 (2021).
10. Soeiro, M. N. C. Perspectives for a new drug candidate for chagas disease therapy. *Mem. Inst. Oswaldo Cruz* **117**, e220004 (2022).
11. Porrás, A. I. *et al.* Target product profile (TPP) for chagas disease point-of-care diagnosis and assessment of response to treatment. *PLoS Negl. Trop. Dis.* **9**(6), e0003697 (2015).
12. Ferreira, L. L. G. & Andricopulo, A. D. World chagas disease day and the new road map for neglected tropical diseases. *Curr. Top. Med. Chem.* **20**(17), 1518 (2020).
13. Goldenberg, S. Chagas disease treatment: A 120-year-old challenge to public health. *Mem. Inst. Oswaldo Cruz* **117**, e210501chgsa (2022).

14. Diaz-Hernandez, A. *et al.* Risk of COVID-19 in Chagas disease patients: What happen with cardiac affectations?. *Biology* **10**(5), 411 (2021).
15. Zaidel, E. J. *et al.* COVID-19: Implications for people with Chagas disease. *Glob. Heart* **15**(1), 69 (2020).
16. Newman, D. J. & Cragg, G. M. Natural products as sources of new drugs over the nearly four decades from 01/1981 to 09/2019. *J. Nat. Prod.* **83**(3), 770 (2020).
17. Londero, V. S. *et al.* Acetylenic fatty acids from *Porcelia macrocarpa* (Annonaceae) against trypomastigotes of *Trypanosoma cruzi*: Effect of octadec-9-ynoic acid in plasma membrane electric potential. *Bioorgan. Chem.* **78**, 307 (2018).
18. Oliveira, E. A. *et al.* Antitrypanosomal activity of acetogenins isolated from the seeds of *Porcelia macrocarpa* is associated with alterations in both plasma membrane electric potential and mitochondrial membrane potential. *J. Nat. Prod.* **82**(5), 1177 (2019).
19. Bousserouel, H., Awang, K., Guéritte, F. & Litaudon, M. Enyne- and enediyne- γ -lactones from the bark of *Meiogyne cylindrocarpa*. *Phytochem. Lett.* **5**(1), 29 (2012).
20. Roque, N. F. & Chaves, M. H. Acetogenins from *Porcelia macrocarpa*: Stereochemical determination of 2-alkyl-3-hydroxyl-4-methyl-(-lactones by ¹³C NMR spectroscopy. *Phytochemistry* **44**(3), 523 (1997).
21. Tiwari, N., Gedda, M. R., Tiwari, V. K., Singh, S. P. & Singh, R. K. Limitations of current therapeutic options, possible drug targets and scope of natural products in control of leishmaniasis. *Mini-Rev. Med. Chem.* **18**(1), 26–41 (2017).
22. Alexandre, T. R. *et al.* Ergosterol isolated from the basidiomycete *Pleurotus salmoneostramineus* affects *Trypanosoma cruzi* plasma membrane and mitochondria. *J. Venom. Anim. Toxins Trop. Dis.* **23**(1), 30 (2017).
23. Chattopadhyay, A. & Jafurulla, Md. A novel mechanism for an old drug: Amphotericin B in the treatment of visceral leishmaniasis. *Biochem. Biophys. Res. Commun.* **416**(1–2), 7 (2011).
24. Morais, T. R. *et al.* Improving the drug-likeness of inspiring natural products—evaluation of the antiparasitic activity against *Trypanosoma cruzi* through semi-synthetic and simplified analogues of licarin A. *Sci. Rep.* **10**(1), 5467 (2020).
25. Koley, D. & Bard, A. J. Triton X-100 concentration effects on membrane permeability of a single HeLa cell by scanning electrochemical microscopy (SECM). *Proc. Natl. Acad. Sci. USA* **107**(39), 16783 (2010).
26. Moreno, S. N. & Docampo, R. Calcium regulation in protozoan parasites. *Curr. Opin. Microbiol.* **6**(4), 359 (2003).
27. Docampo, R. & Huang, G. Calcium signaling in trypanosomatid parasites. *Cell Calcium* **57**(3), 194 (2015).
28. Docampo, R. & Moreno, S. N. J. Acidocalcisomes. *Cell Calcium* **50**(2), 113 (2011).
29. Vannier-Santos, M., Martiny, A. & Souza, W. Cell biology of *Leishmania* spp.: Invading and evading. *Curr. Pharm. Des.* **8**(4), 297 (2002).
30. Kaczanowski, S., Sajid, M. & Reece, S. E. Evolution of apoptosis-like programmed cell death in unicellular protozoan parasites. *Parasit. Vectors* **4**(1), 44 (2011).
31. Amaral, M. *et al.* A semi-synthetic neolignan derivative from dihydrodieugenol B selectively affects the bioenergetic system of *Leishmania infantum* and inhibits cell division. *Sci. Rep.* **9**(1), 6114 (2019).
32. Tirichen, H. *et al.* Mitochondrial reactive oxygen species and their contribution in chronic kidney disease progression through oxidative stress. *Front Physiol.* **12**, 627837 (2021).
33. Strzycz, P. ATP and ROS signal cell extrusion. *Nat. Rev. Mol. Cell Biol.* **23**(6), 387 (2022).
34. Brookes, P. S., Yoon, Y., Robotham, J. L., Anders, M. W. & Sheu, S. S. Calcium, ATP, and ROS: A mitochondrial love-hate triangle. *Am. J. Physiol. Cell Physiol.* **287**(4), C817 (2004).
35. Silva, M. L., Costa-Silva, T. A., Antar, G. M., Tempone, A. G. & Lago, J. H. G. Chemical constituents from aerial parts of *Baccharis sphenophylla* and effects against intracellular forms of *Trypanosoma cruzi*. *Chem. Biodiv.* **18**, 10 (2021).
36. Galhardo, T. S. *et al.* New derivatives from dehydrodieugenol B and its methyl ether displayed high anti-*Trypanosoma cruzi* activity and cause depolarization of the plasma membrane and collapse the mitochondrial membrane potential. *Chem. Biol. Interact.* **366**, 110129 (2022).
37. Londero, V. S. *et al.* Anti-*Trypanosoma cruzi* activity of costic acid isolated from *Nectandra barbellata* (Lauraceae) is associated with alterations in plasma membrane electric and mitochondrial membrane potentials. *Bioorg. Chem.* **95**, 103510 (2020).
38. Umehara, E. *et al.* Differential lethal action of C17:2 and C17:0 anacardic acid derivatives in *Trypanosoma cruzi*—a mechanistic study. *Bioorgan. Chem.* **102**, 104068 (2020).
39. Costa-Silva, T. A., Silva, M. L., Antar, G. M., Tempone, A. G. & Lago, J. H. G. Ent-Kaurane diterpenes isolated from n-hexane extract of *Baccharis sphenophylla* by bioactivity-guided fractionation target the acidocalcisomes in *Trypanosoma cruzi*. *Phytomedicine* **93**, 153748 (2021).
40. Mukherjee, S. B., Das, M., Sudhandiran, G. & Shaha, C. Increase in cytosolic Ca²⁺ levels through the activation of non-selective cation channels induced by oxidative stress causes mitochondrial depolarization leading to apoptosis-like death in *Leishmania donovani* promastigotes. *J. Biol. Chem.* **277**(27), 24717 (2002).
41. Romanelli, M. M. *et al.* Mitochondrial Imbalance of *Trypanosoma cruzi* Induced by the marine alkaloid 6-bromo-2'-de-N-methylaplysinopsin. *ACS Omega* **7**(32), 28561 (2022).

Acknowledgements

The authors would like to thank São Paulo Research Foundation—FAPESP (Projects 2020/01221-4, 2021/02789-7 and 2021/04464-8), CAPES (financial code 001) and the National Council for Scientific and Technological Development—CNPq (301354/2019-4 and 405691/2021-1) for the financial support. This publication is part of the activities of the Research Network Natural Products against Neglected Diseases (ResNetNPND): <http://www.uni-muenster.de/ResNetNPND/>.

Author contributions

F.T., I.A.B. and J.H.G.L. contributed to chromatographic procedures and chemical characterization. F.T., T.A.C.S., A.G.T. and J.H.G.L. contributed to the manuscript preparation. T.A.C.S. and A.G.T. contributed to the bioactivity tests and mechanism of action studies. All authors read, revised, and approved the manuscript.

Competing interests

The authors declare no competing interests.

Additional information

Supplementary Information The online version contains supplementary material available at <https://doi.org/10.1038/s41598-023-37520-3>.

Correspondence and requests for materials should be addressed to A.G.T. or J.H.G.L.

Reprints and permissions information is available at www.nature.com/reprints.

Publisher's note Springer Nature remains neutral with regard to jurisdictional claims in published maps and institutional affiliations.



Open Access This article is licensed under a Creative Commons Attribution 4.0 International License, which permits use, sharing, adaptation, distribution and reproduction in any medium or format, as long as you give appropriate credit to the original author(s) and the source, provide a link to the Creative Commons licence, and indicate if changes were made. The images or other third party material in this article are included in the article's Creative Commons licence, unless indicated otherwise in a credit line to the material. If material is not included in the article's Creative Commons licence and your intended use is not permitted by statutory regulation or exceeds the permitted use, you will need to obtain permission directly from the copyright holder. To view a copy of this licence, visit <http://creativecommons.org/licenses/by/4.0/>.

© The Author(s) 2023